

Performance and Emission Study on Diesel Engine using Biofuel as Substitute with RSM

Moshiha K S¹, Kanthavelkumaran N^{2*}, Prasanth P V², Seenikannan P³, Bibin C⁴

¹ PG Scholar, Thermal Engineering, Ponjesly College of Engineering, Nagercoil, Tamilnadu, India

² Mechanical Engineering, Ponjesly College of Engineering, Nagercoil, Tamilnadu, India

³ Mechanical Engineering, AAA College of Engineering, Amathur, Sivakasi, Tamilnadu, India

⁴ Mechanical Engineering, RMK College of Engineering and Technology, Chennai, Tamilnadu

* Corresponding Author: kanthavelpriya@gmail.com

Abstract. -The crucial justification this examination article is to break down the combined effects of biodiesel-ethanol fuel blends on the display and surge ascribes of a diesel engine by the Response Surface Methodology. Considering the results, the brake power and power were lessened by around 29% with growing the proportion of ethanol in the fuel mix. Maybe then, the BSFC of fuel blends improved around 15% in with a more elevated level of ethanol in light of the lesser calorific assessment of ethanol related with biodiesel. Regardless, higher thickness and thickness of biodiesel premise extra fuel implantation; so there is no perceptible change in BSFC regards for all blends. About spread limits, the more degree of ethanol achieved less proportion of smoke level and NO_x release around 38% and 17%, independently in view of the incredible level of oxygen in the nuclear development of ethanol. Regardless, there is an around 44% diminishing in CO outpourings for a significant degree of biodiesel contained blends. As shown by the GA smoothing out, the results showed that the biodiesel rate in the fuel mix, RPM, and engine trouble were joined to 94.65%, 2800, and 65.75%, in a particular request as the ideal conditions. It is assumed that ethanol is more suitable to improve the spread ascribes than that of the introduction characteristics.

Keywords — *Alternative fuels; Blend of Bio-diesel; Emission Characteristics; Response Surface Methodology; Environment Safety*

I. INTRODUCTION

In view of rising requests for energy especially in Asia and the Middle East and vaporous contamination issues, it is expected to discover elective fuel sources and clarifications for inside burning motors [1]. Consequently, biomass sources generally biofuels, for example, biodiesel and bioethanol are standing out enough to be noticed these years [2]. Vegetable root biofuels were viewed as supportive among the sources because of their high biodegradability and lubricity, which has been the principle worry in present day motor ignition [3]. Biodiesel is a type of diesel fuel got from plants or creatures and comprising of long-chain unsaturated fat esters. Bioethanol is an oxygen content fuel that can be delivered from agrarian waste and blackstrap molasses feedstock [4]. Bioethanol is an oxygen content fuel that can be delivered from horticultural waste and molasses feedstock [5]. In any case, lower cetane file and helpless solvency of ethanol contrasted and diesel fuel cause numerous specialized limits to the immediate utilization of ethanol in chilly climate conditions [6]. Directed outflows

like nitrogen oxide (NO_x), carbon monoxide (CO), and smoke number are the fundamental sorts of discharges in the fumes of diesel motors. Carbon monoxide is harmful to people and creatures when met in higher focuses. Nitric oxide (NO) and nitrogen dioxide (NO₂) as NO_x discharges framed all through the burning of fills in engine vehicles, private, motors, and other hardware. There are numerous examinations associated with the improvement of the presentation and discharge qualities of diesel motors fuelled with biodiesel-diesel mixes [7].

Some of them are accounted for in the underneath lines: Singh et al. [8] researched the impact of Jatropha biodiesel through transesterification response with the utilization of a heterogeneous impetus. The outcomes showed that the presentation of the motor fuelled with B20 was practically equivalent to that of diesel fuel. Additionally, a significant decline in HC outflows (14.3%) identified with diesel, and a slight expansion in NO_x discharges (2%) was likewise noticed. Motor working boundaries improvement has been executed utilizing the focal composite plan technique (CCD) by Elkelawy et al. [9] to accomplish an ideal break

warm effectiveness of a solitary chamber DI-motor filled by biodiesel-diesel blends. RSM analyzer results demonstrated that the most ideal estimations of BTE, UHC, and NO_x were 13.656%, 120.7748 ppm, and 234.8926 ppm, separately, at the maximum estimation of biodiesel combination of 70% and brake force of 2.05 kW. In another examination [10], the impacts of utilizing B20 and B50 mixes of diesel-biodiesel energized blended in with three unique convergences of the Acetone as an oxygenated natural compound were explored in a diesel motor. The outcomes acquired for B20 with 2% CH₃CO showed that the Brake Thermal Efficiency (BTE) was improved by 12.64% when contrasted and the business diesel fuel. Also, there are a decrease of 18.09% and 11.22% for the fumes gas temperature and explicit energy utilization, individually. Carbon monoxide (CO), Carbon dioxide (CO₂), UHC, and Particulate matter discharges were diminished drastically by 63.38%, 22.69%, 47.76%, and 40.84%. Elkelawy et al. [11] arranged three diesel-biodiesel Blends with Mn (II) supramolecular complex nanoparticle emulsions. The outcomes showed that the tasks of the motor in the presence by utilizing nanofluid emulsions improved the warm brake effectiveness by 15–20% contrasted and diesel fuel. Besides, CO and HC emanations are altogether diminished by 49–62% and 15–61% contrasted with unadulterated diesel fuel, separately. It is seen that the NO_x discharges for all nanofluids ignition increment by 30–68% and the smoke outflows decrease by 32–44% in correlation with unadulterated Diesel. In any case, a little exploration was done on the utilization of biodiesel/ethanol mixes in diesel motors. Wei et al.

Zheng et al. [12] performed examination to explore the effects of biodiesel-n-butanol, biodiesel-ethanol, and biodiesel-2,5-dimethylfuran mixes on the burning and emanations on a diesel motor. The outcomes showed that the ITE of a motor energized with biodiesel-diesel mixes was lower than that of diesel fuel at low motor burdens. The creators revealed that biodiesel-diesel mixes had higher ITE than that of perfect diesel fuel, particularly with expanding motor burden at EGR rates. The outcomes likewise showed that slick biodiesel, n-butanol, and 2,5-dimethylfuran mixes delivered higher NO_x emanations contrasted with perfect diesel, while ethanol had lower NO_x discharges. The consequences of this exploration additionally showed that warm proficiency and smoke improved at high motor burden by expanding the measure of biodiesel, n-butanol, and 2,5-dimethylfuran. Zheng et al. [13] researched the impact of n-butanol, 2,5-dimethylfuran, and ethanol mixes on the outflows and burning qualities of a RCCI diesel motor. The outcomes showed that biodiesel-ethanol mixes had longer start delay than different powers and this fuel mix demonstrated a lower NO_x and residue discharges. Then again, biodiesel-n-butanol created the most elevated showed warm productivity under RCCI ignition. Tutak et al.

[14] played out an investigation to look at the impact of burning, discharge and, the presentation of diesel-ethanol and biodiesel-ethanol fuel mixes with the volumetric portion up to 45% for ethanol on a one-chamber diesel motor. The outcomes showed that the most noteworthy ITE esteem was accomplished for the diesel-ethanol mix, mix included 35% of the ethanol. Also, the greatest estimation of NO_x was acquired for the diesel-ethanol mix included 70% of diesel. The outcomes additionally showed that THC emanations improved up to around 40% of the ethanol extent in the fuel blend. Madiwale et al. [5] introduced a trial study to examine the impact of ethanol expansion to biodiesel-diesel mixes on the exhibition of a solitary chamber motor. The aftereffects of execution showed that brake force and BTE improved by the expansion of ethanol to biodiesel-diesel mixes while BSFC expanded at different burdens. Hu et al. [15] introduced an exploratory examination to assess the discharges attributes of a diesel motor powered with the ethanol-biodiesel-diesel mixes. The consequences of unstable natural mixtures discharges showed that ethanol-biodiesel-diesel combination expanded complete emanations around 85% at the greatest force yet it diminished by 15% and 21% at 10% and half motor burdens, separately contrasted and diesel. The unstable natural mixtures discharges of the ethanol-biodiesel-diesel mix were improved contrasted with flawless diesel at medium and low motor burdens.

Aydin and İlkılıç [16] utilized ethanol as an added substance to investigate the conceivable utilization of higher rates of biodiesel in an unmodified diesel motor. 20% biodiesel and 80% diesel fuel and 80% biodiesel (BE20) and 20% ethanol were utilized in a solitary chamber diesel motor. The impact of test fills on motor force, force, and brake explicit fuel utilization, brake warm productivity, fumes gas temperature, and CO, CO₂, NO_x, and SO₂ outflows was explored. The exploratory outcomes showed that the presentation of the CI motor was improved with the utilization of the 80% biodiesel and 20% ethanol fuel mix in contrast with 20% biodiesel and 80% diesel fuel mix. Also, the exhaust outflows for BE20 were genuinely diminished. As per the writing survey, ordinarily the measure of ethanol in diesel-biodiesel-ethanol mix is 5 to 20%, nonetheless, a few scientists utilized 30 to half ethanol in diesel-biodiesel-ethanol mix [17]. Additionally, a few investigations utilized 50 to 80% ethanol in ethanol-diesel mixes [18]. Be that as it may, the greatest measure of ethanol in the biodiesel-ethanol mixes is 45% as was referenced in the presentation. To beat high cost, exorbitant, and tedious test approach admonishes, the utilization of the fluffy rationale framework and fake neural organization and RSM methods help in the legitimate expectation of information with high precision that outline the genuine outcomes [19]. Reaction surface procedure is a social event of the factual based numerical strategies which is among the most applicable multivariate

methods for motor displaying. Reaction surface strategy additionally gauges the get together among the overseeing motor information factors and the subsequent yield reactions of the motor [20]. Besides, a few enhancement methods have been created and utilized in motor execution and outflow boundaries improvement. Old style improvement strategies force a few constraints on addressing numerical programming models. In light of this inspiration, nature-enlivened calculations like Genetic Algorithm (GA), Simulated Annealing (SA), and Tabu Search (TS) can be given more consideration. Writing surveys showed that there are so far no explores zeroed in on the examination of the consolidated impacts of utilizing biodiesel-ethanol mixes and different motor velocities and burdens on the presentation and discharge attributes of a diesel motor. Besides, there isn't any conversation about enhancement in these examinations that thinks about ethanol and biodiesel rate in the fuel blend, motor speed, and burden. As a development, no exploration works were depicted in motor examinations with a high level of ethanol (half) in the fuel blend. Along these lines, the goal of this exploration paper is the streamlining and examination of the impacts of biodiesel-ethanol mixes on the exhibition and emanation qualities of a diesel motor. Reaction Surface Methodology (RSM) was applied to create numerical connections between autonomous factors and brake power, force, BSFC, CO, NO_x emanations, and smoke level as the reactions. Also, thermo-actual properties and motor in-chamber pressure for different fuel mixes were researched and contrasted and one another. At last, the presentation and emanation boundaries of the motor fuelled with a biodiesel-ethanol mix and flawless diesel were thought about.

II. MATERIALS AND METHODS

A. Biodiesel preparation and Fuel properties

In the current examination, biodiesel was delivered from squander cooking oil by transesterification response

utilizing methanol and potassium hydroxide (KOH) tablets as the liquor and impetus separately. Titration was performed to decide the measure of KOH expected to kill the free unsaturated fats in squander cooking oil. The measure of KOH required as an impetus was resolved as 0.98 mg/g Oil. The biodiesel was acquired at a response temperature of 55oC, 6:1 liquor to oil molar proportion, and response season of 85 min. additionally; ethanol utilized in this investigation was bought from a neighborhood provider with 99% virtue. The energizes were blended by hand in the holders. The significant properties of cooking oil methyl ester (biodiesel) and ethanol and fuel mixes acquired from the ASTM technique are appeared in Tables 1 and 2, individually.

B. Test Engine

An immediate infusion and water-cooled diesel motor has been utilized for the test tests. The determinations of the motor are introduced in Table 3. The motor run with different biodiesel-ethanol mixes at the diverse motor rates and loads as per the grid of analyses. Fig. 1 shows a schematic chart of the motor arrangement and control board. The motor was coupled to a whirlpool current dynamometer (E400) and an AVL gas analyzer (DiCom 4000) was utilized to quantify outflow boundaries. Smoke meter AVL Di Smoke 4000 is utilized to gauge the channel smoke level. The motor was permitted to run a couple of times until the cooling water and the greasing up oil temperature arrive at 80 °C and afterward the information were recorded. The pressing factor sensor (Kistler) was used to quantify the burning pressing factor (Table 4). The chamber pressure information were recorded in 1°crank-point increase. For each working point, the chamber pressing factors of 50 cycles were gathered.

Table 1 Properties of biodiesel and ethanol fuels used for the present study

Property	Method	Units	Biodiesel	Ethanol
Kinematical viscosity, 40 °C	ASTM-D445	mm ² /s	4.15	1.2
Density at 20 °C	–	kg/m ³	850	800
Lower calorific value	ASTM-D240	kJ/kg	38,800	26,800
Cetane number	ASTM-D613	–	63	8
Oxygen content	–	wt%	11	34.8
Carbon content	–	wt%	77	52

Table2 Thermo-physical properties of the fuel blends:

Property	Unit	B50E50	B60E40	B75E25	B90E10
Kinematic viscosity(40°C)	Mm ² /s	2.4	2.62	3.17	3.58
Density					
Lower calorific value	g/cm ³	825	830	838	845
Cetane number	kJ/kg	32,800	34,000	35,800	37,600
	-	38	43	50	59

Table 3 Engine specifications

Cylinder number	4
Compression ratio	16:1
Stroke(mm) x Bore(mm)	128 x 97
Maximum Power	82 Kw at 2800 RPM
Maximum Torque	350 N.m at 1800 RPM

C. Design of Experiment and Analysis

The Experimental design performed by Design-Expert software v7 according to the RSM using the central composite design (CCD) to report the relationship between the response and independent variables. The independent parameters were defined as the biodiesel percentage in fuel mixture (X₁), engine speed (X₂), and engine load (X₃) according to Table 5. The six responses (Y) were power, torque, brake specific fuel consumption, NO_x, CO emission, and smoke level. Based on the RSM method (CCD) for three independent variables α is 1.682, and in the experimental data matrix (Table 5), the rows 6, 7, 8, 15, 19 and 20 should be repeated. The response functions were extracted according to the second-order polynomial equation based on Eq. (1) [38]:

$$y = b_0 + b_1x_1 + b_2x_2 + b_3x_3 + b_{11}x_1^2 + b_{22}x_2^2 + b_{33}x_3^2 + b_{12}x_1x_2 + b_{13}x_1x_3 + b_{23}x_2x_3 \quad \text{-----(1)}$$

D. Uncertainty Analysis

The uncertainties of the experimental parameters are affected by different error sources, namely, the random

fluctuation of employed instruments, the calibration of the test bed, and the observation accuracy [4]. For directly measured parameters, the measurement uncertainties are defined by the accuracies of the experimental instruments. For computed parameters, the measurement uncertainties are determined based on the principle of the root-mean-square method and the measurement accuracies of the measured parameters [39,40]:

$$e_R = \left[\left(\frac{\partial f}{\partial X_1} e_{e1} \right)^2 + \left(\frac{\partial f}{\partial X_2} e_{e2} \right)^2 + \dots + \left(\frac{\partial f}{\partial X_n} e_{en} \right)^2 \right]^{1/2} \quad \text{----- (2)}$$

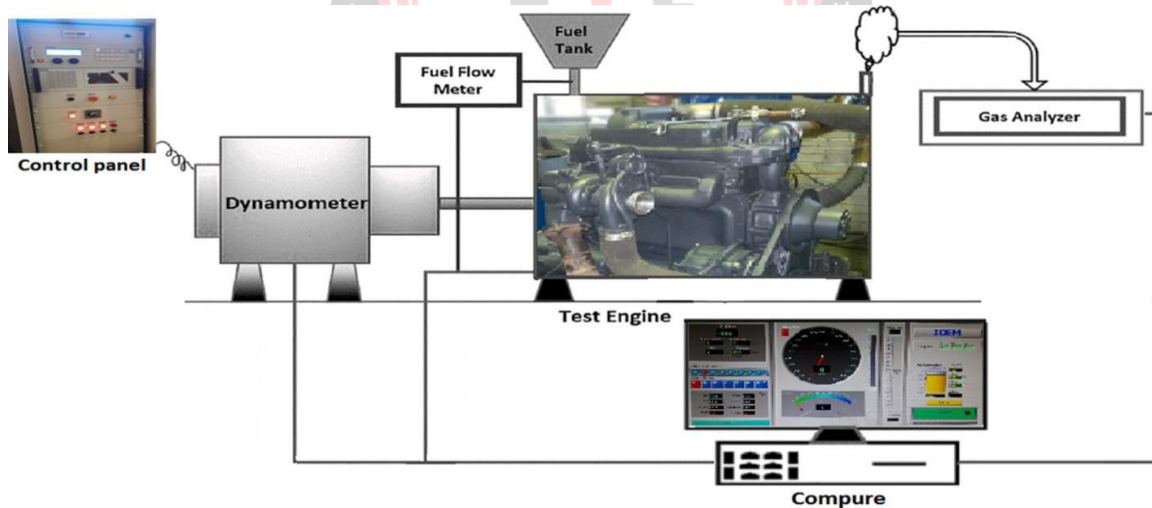


Fig. 1. The schematic diagram of the engine set up and control panel.

Table 4 Technical specifications of the in-cylinder pressure sensor.

Model	6613CA
Measurement range	0-250 bar
Sensitivity	10-mV/bar
Sensitivity to acceleration	0.001 bar/g

Table 5 The central composite experimental design matrix.

Experiment number	Percentage of biodiesel in the biodiesel-ethanol mixture (%) X ₁	Engine speed(rpm) X ₂	Engine load (%) X ₃
1	60	1365	40
2	90	1365	85
3	100	1900	25
4	75	1900	62.5
5	90	2435	85
6	75	1900	62.5
7	75	1000	62.5
8	75	1900	62.5
9	75	1900	62.5
10	75	1900	100
11	60	1365	85
12	50	1900	62.5
13	90	1365	40
14	90	2435	40
15	75	1900	62.5
16	60	2435	40
17	75	2800	62.5
18	60	2435	85
19	75	1900	62.5
20	75	1900	62.5

Table 6 The accuracies and uncertainties of the measurements and calculated parameters.

Measured parameter	Measurement range	Accuracy of measurement
Speed	0-2500 rpm	±1 rpm
Fuel flow rate		±0.1%
CO	0-10%	0.01 vol%±
NO _x	0-5000 PPM	±5% reading
HC	0-2000 PPM	±3% reading
Soot opacity	0-100%	±0.1%
Torque	0-400Nm	±0.5%
Calculated parameter		Uncertainty in the computation
Brake power	-	±0.263kW
BSFC	-	±1.216 gr/kWh

III. ANALYSIS AND RESULTS

Figs. 2 to 5 show the changes in kinematic viscosity, density, lower calorific value, and cetane number properties with the biodiesel-ethanol blend relative to neat biodiesel fuel, respectively. The results indicated that the addition of ethanol in the fuel mixture reduces the entire thermo-physical properties of the blends. Based on the results the kinematic viscosity decreases by around 42% when the amount of ethanol in the fuel mixture is 50% in comparison with B100. However, there is a 14% reduction for B90E10 compared with neat biodiesel. According to the results, the minimum reduction (0.6%) in density belongs to B90E10 while the maximum

decrement (3%) occurs for B50E50 relative to neat biodiesel fuel. Moreover, the minimum and maximum reduction in lower calorific value belong to B90E10 and B50E50 fuel blends with the amount of 3 and 16% compared with neat biodiesel, respectively. The results indicate that B50E50 has the highest reduction (40%) in cetane number and the lowest decrease (6.5%) in this property belongs to the B90E10 blend with respected to B100. As the results show, the addition of ethanol has more influence on kinematic viscosity and cetane index in comparison with the other two properties.

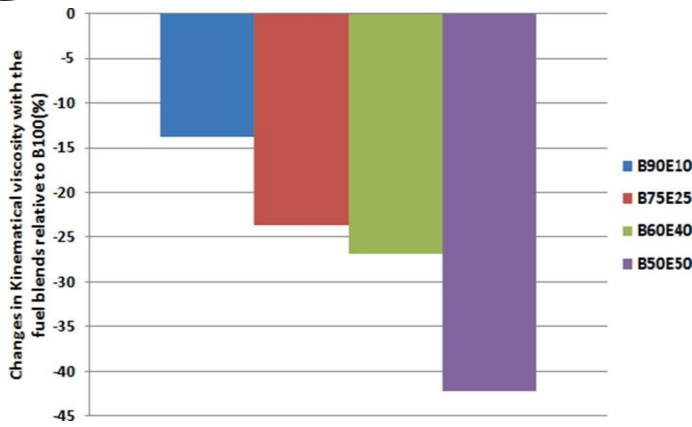


Fig. 2. Changes in kinematic viscosity with the biodiesel-ethanol blends relative to neat biodiesel

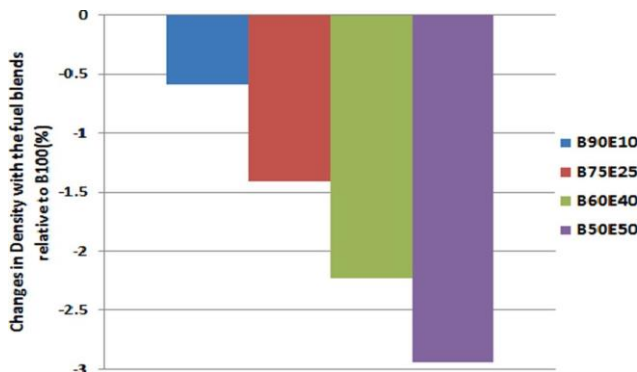


Fig. 3. Changes in density with the biodiesel-ethanol blends relative to neat biodiesel.

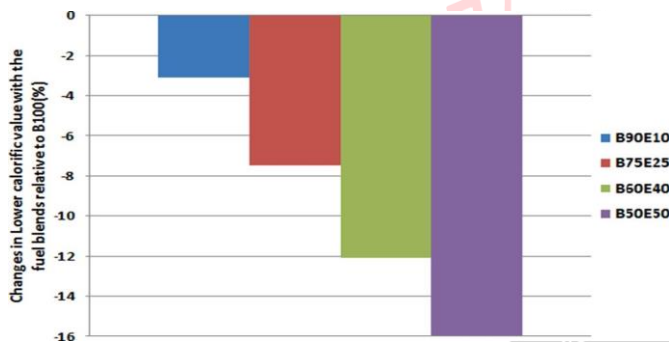


Fig. 4. Changes in lower calorific value with the biodiesel-ethanol blends relative to neat biodiesel

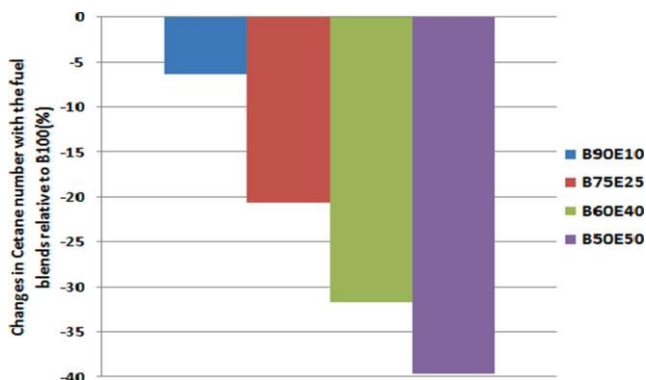


Fig.5.Changes in cetane number with the biodiesel-ethanol blends relative to neat biodiesel

A. Engine in-cylinder pressure for various fuel blends

Fig. 6 shows the variety of in-chamber (burning) pressure versus wrench plot for B90E10, B75E25, B60E40, and B50E50 fuel mixes at the motor speed of 1900 RPM and

full motor burden. Fig. 6 shows that, as a rule, the mixed fills including higher biodiesel rate lead to higher in-chamber pressure. It very well may be because of the greater warming estimation of the biodiesel that causes higher in-chamber pressure. Another explanation is the higher cetane number of biodiesel contrasted and ethanol that brought about before burning and more opportunity to happen total burning because of its more limited start delay [4,21]. Nonetheless, the greatest in-chamber pressure fluctuates with expanding ethanol fixation due to delayed the start defer which could move the ignition cycle away from the TDC. Then again, the premixed consume segment of ethanol is more prominent than that of biodiesel. This marvel came about because of the predominant vanishing rate and longer start postponement of ethanol which give improved fuel-air blending during the premixed consume stage that brought about the most noteworthy pinnacle of in-chamber pressure for B50E50 among all fuel mixes [15,22].

B. Statistical analysis

The coefficients of relapse models, R2, and p-values for every reliant variable were introduced in Table 7. Also, the test and model information were contrasted with approve the numerical models (Fig. 7). The examination showed that the proposed models were satisfactory, with no absence of fit and with adequate estimations of R2 for every one of the autonomous factors (reactions). The numerical models were likewise approved with an examination of the anticipated information extricated by the models and exploratory information. As per the outcomes, the models' information are as per the test information which shows the ideal attack of the models and reasonable connection got between the factors.

C. Brake Power

The anticipated estimations of brake power for different mixes and motor paces are introduced in Figs. 8 to 10. As the figures show the brake power expanded with expanding the measure of biodiesel in the fuel mix. As indicated by the outcomes, the brake power diminished by 30% with a higher part of ethanol in the fuel blend. The primary justification this conduct could be because of the decrease of the calorific estimation of the mixes containing ethanol. Furthermore, the higher cetane record of biodiesel which causes more limited start deferral and longer burning length serves to more finish ignition. These outcomes concur well with past examinations [23]. The outcomes showed that the brake power upgrades at high motor rates because of the expanded atomization and gulf wind current that makes a more homogeneous blend.

Additionally, the higher oxygen substance of ethanol than that of biodiesel gives more complete burning conditions particularly at high motor loads, and remunerates the

lower of the warmth substance of ethanol. As indicated by the figures, the brake power expanded at higher motor loads because of more complete ignition conditions because of the great burning temperature and better blending of biodiesel and ethanol as the oxygenated powers with the air atoms that produce more complete ignition and improves the brake power as different papers have revealed [13,15,24]. Nonetheless, the expansion of ethanol in fuel combination prompts a lower burning temperature at fractional loads because of the lean in general blend and causes a slight decrease in the motor force.

D. Force

Figs. 11 to 13 demonstrate the effects of different biodiesel-ethanol mixes and motor speed on the anticipated motor force at various motor burdens. As indicated by the figures, the most extreme force has a

place with the mixes containing over 70% WCO methyl ester at the motor speed somewhere in the range of 1800 and 2000 RPM. Additionally, the base force happens at the motor speed higher than 2400 for the mixes included <60% biodiesel.

The outcomes likewise showed that the anticipated qualities for motor force diminished roughly 27% with the increment of ethanol portion in the fuel blend because of the lower heat substance of ethanol in correlation with biodiesel. Additionally, high lubricity and more limited start postponement of biodiesel bring about lower grinding conditions and better burning productivity which upgrades the motor force. The outcomes are in concurrence with different examinations. The figures show the motor force improves with the expanded motor burden because of the more complete ignition under the higher motor burdens.

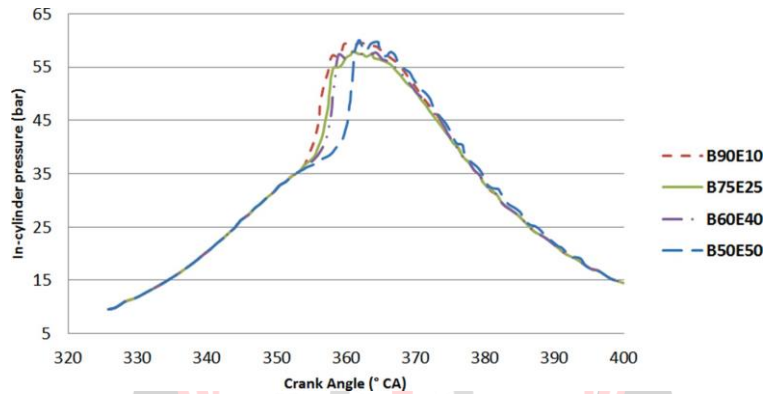


Fig. 6. In-cylinder pressure variations versus crank angle at full engine load.

Table 7 Coefficients, p-values, and R2 for the emission parameters of the engine.

Regression coefficient	Brake power (kW)	Brake torque (N.m)	BSFC (gr/kW.hr)	Smoke (Soot opacity %)	CO (%)	NOx (ppm)
b ₀	-62.431	-569.468	405.096	0.013115	+0.1528	322.673
b ₁	0.61788	6.04433	-0.50376	0.39570	- 1.1601 × 10 ⁻⁰³	-4.6274
b ₂	0.048030	0.32961	-0.091181	-4.71779 × 10 ⁻⁰³	-3.19118 × 10 ⁻⁰⁵	0.17323
b ₃	0.10836	4.29054	-1.15810	-0.097499	-1.01046 × 10 ⁻⁰³	0.8397
b ₁₂	2.0899 × 10 ⁻⁰⁴	1.257 × 10 ⁻⁰⁴	-3.6141 × 10 ⁻⁰⁴	-8.32815 × 10 ⁻⁰⁵	-	-2.04275 × 10 ⁻⁰⁴
b ₁₃	4.5632 × 10 ⁻⁰³	0.014331	6.713 × 10 ⁻⁰³	1.01823 × 10 ⁻⁰³	-	-1.13137 × 10 ⁻⁰³
b ₂₃	2.839 × 10 ⁻⁰⁴	-2.0951 × 10 ⁻⁰⁵	2.095 × 10 ⁻⁰⁵	-2.61891 × 10 ⁻⁰⁵	1.46659 × 10 ⁻⁰⁷	-1.87514 × 10 ⁻⁰³
b ₁₁	-6.766 × 10 ⁻⁰³	-0.0389	1.417 × 10 ⁻⁰³	-7.86970 × 10 ⁻⁰⁴	5.02751 × 10 ⁻⁰⁶	0.045575
b ₂₂	- 1.6578 × 10 ⁻⁰⁵	-9.0566 × 10 ⁻⁰⁵	3.668 × 10 ⁻⁰⁵	1.92363 × 10 ⁻⁰⁶	3.87925 × 10 ⁻⁰⁹	-5.37232 × 10 ⁻⁰⁵

b ₃₃	-1.229 × 10 ⁻⁰³	-0.01803	1.681 × 10 ⁻⁰³	1.17912 × 10 ⁻⁰³	4.36778 × 10 ⁻⁰⁶	0.055811
R ²	96.5%	98.7%	95.6%	99.3%	95.7%	94.5%
p-value	<0.001	<0.001	<0.001	<0.001	<0.001	<0.001

E. Brake specific fuel consumption (BSFC)

Figs. 14 to 16 demonstrate the effects of different biodiesel-ethanol mixes and motor speed on the anticipated BSFC at different motor burdens. As indicated by the figures, the greatest BSFC (around 320 g/kW. h) has a place with the mixes containing under 55% biodiesel under motor speed of 2700 to 2800 RPM. Likewise, the base BSFC (<210 g/kW.h) happened under motor speed of 1500 to 1700 RPM for the mixes included <10% biodiesel. In light of the plots, from the start, the BSFC esteems dropped with the speed up to 1600 RPM and afterward expanded pointedly at the rates of in excess of 1800 rpm. The anticipated qualities for the BSFC expanded (roughly 16%) with the expanding ethanol extent in the fuel mix. Given that BSFC is straightforwardly identified with brake power so the lower calorific estimation of the ethanol in examination with biodiesel that causes lower brake power and thusly higher BSFC. As the figures show, the BSFC diminishes with an increment in the motor burden. It very well may be because of improving the brake power when contrasted with fuel utilization in these conditions. In addition, the significant level oxygen of ethanol can take part in the burning interaction at higher motor loads and improves ignition conduct to decrease BSFC at this condition. The outcomes were found to concur with different examinations [12, 24, 26].

F. Brake Specific Energy Consumption (BSEC)

BSEC (Brake Specific Energy Consumption) is the proportion of energy acquired by consuming fuel for an hour to the genuine energy or brake power. This boundary decides how successful the energy is changed over from fuel. It is characterized as a result of BSFC and calorific estimations of fuel. It implies how productively fuel energy is acquired from given fuel.

Figs. 17 to 19 show the effects of different biodiesel-ethanol mixes and motor speed on the anticipated BSEC at different motor burdens. As per the figures, at high motor paces the BSEC diminishes with expanding biodiesel mixing rate for all heap states of the motor because of lower brake explicit fuel utilization of biodiesel. Nonetheless, at lower motor rates there is no huge distinction in BSEC between fuel mixes which infers that the higher calorific estimation of biodiesel contrasted and ethanol repays the lower BSFC of biodiesel at this motor condition. As the figures show, the BSEC diminishes with an increment in the motor burden.

G. Smoke Level

The anticipated smoke levels (sediment obscurity rate) for different mixes and motor rates are demonstrated in Figs. 20 to 22. The figures show smoke level in the fumes gas diminished (around 38%) with the expanding ethanol portion in the fuel blend. The principle reason is the higher oxygen atoms and less C-C bonds in the liquor structure that causes more oxidation and less residue arrangement and motor running in generally speaking more slender zones. As indicated by the figures, the smoke level abatements with the speeding up because of better fuel atomization and more disturbance in the burning chamber that creates a more homogeneous combination and diminishes smoke level. Comparative outcomes can be found in different investigations. As demonstrated in figures, there is an expanded residue development at higher motor burdens as a result of high gas temperatures in the chamber that prompts a more atomic pace of impacts.

H. CO emissions

Figs. 23 to 25 show the CO emanation esteems for different mixes. It tends to be seen the CO discharges diminished by up to 44% with expanding the biodiesel rate in the fuel combination. This diminishing might be because of the lower start deferral of the biodiesel that causes more complete burning. Then again, impeded burning staging and lower adiabatic fire temperature of ethanol watch out for low ignition temperature particularly at lower motor loads and produce more carbon monoxide [27]. The outcomes likewise showed that the distinction between the carbon monoxide esteems with speeding up at low and medium burdens is more prominent than at high loads. As indicated by the outcomes, the CO discharges diminished for all mixes with speeding up due to better burning conditions because of higher blending air and fuel and higher ignition temperature. It is in concurrence with different examinations [27]. Likewise, the CO emanations are higher at lower motor loads because of the low ignition temperature of ethanol at lower motor loads that cause higher discharge of carbon monoxide. It was called attention to by different analysts [14]. Also, at low motor burdens, terrible atomization conditions because of the great consistency of biodiesel lead to an increment in CO outflow. Be that as it may, under higher motor loads, the ethanol causes better infusion of the mixes joined by to cut down the consistency of the biodiesel and separate the hydros of the powers into more modest components during ignition. This detachment permits the oxygen particles of ethanol and biodiesel to take an interest in the burning;

accordingly the CO emanation diminishes in rich zones at higher motor burdens.

I. NOx emissions

The anticipated NOx outflow for different mixes and motor paces are demonstrated in Figs. 26 to 28. As indicated by the figures, NOx discharges diminished with a speed up. This is a direct result of less home season of the pinnacle temperature of the burning gas because of the more limited start defer that causes an improvement in NOx emanation. In any case, the distinction in NOx esteems for different biodiesel-ethanol mixes at lower motor rates is more prominent than that at high motor rates.

Figures additionally show that the NOx emanations declined (roughly 17%) with a higher level of ethanol in the fuel blend in concurrence with the consequences of different papers [28]. This conduct could be because of lower temperatures conditions during the ignition of the mixes included ethanol because of lower cetane number, calorific worth, and adiabatic fire temperature of ethanol and its higher dormant warmth. Then again, the higher burning temperature of biodiesel is the consequence of its higher warming worth and the presence of oxygen atoms in its construction that cause a more elevated level of NOx outflows. As indicated by figures, the NOx development expanded with the expanded motor burden for all mixes because of an expansion in fumes gas temperature.

J. Optimization

In this study, there were three decision parameters namely the biodiesel percentage, engine speed, and load. The following limitations are applied to the decision parameters according to the design of the experiment:

$$50 \leq \text{Biodiesel} \leq 100$$

$$1000 \leq \text{RPM} \leq 2800$$

$$25 \leq \text{Load} \leq 100$$

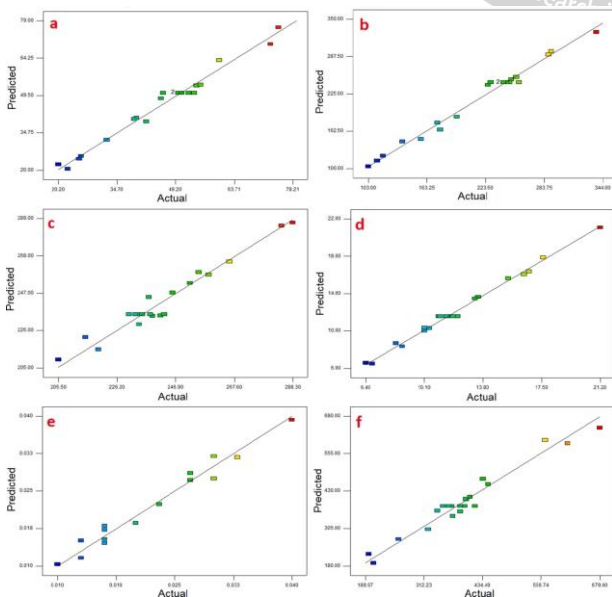


Fig. 7. Predicted values versus actual values of a) brake power b) brake torque c) BSFC d) Smoke level e) CO and f) NOx.

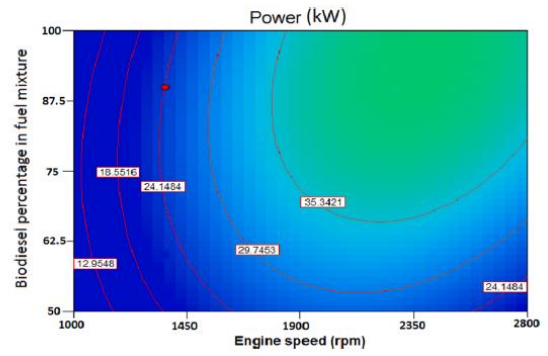


Fig. 8. Brake power versus engine speed at 40% load.

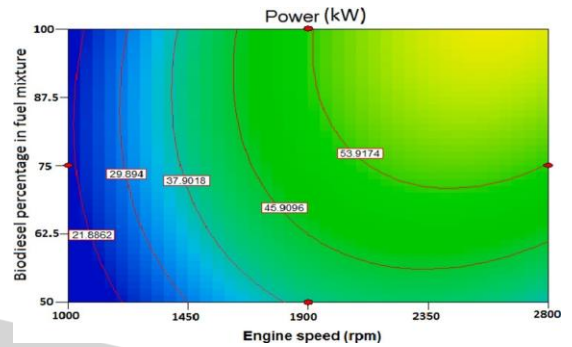


Fig. 9. Brake power versus engine speed at 62.5% load.

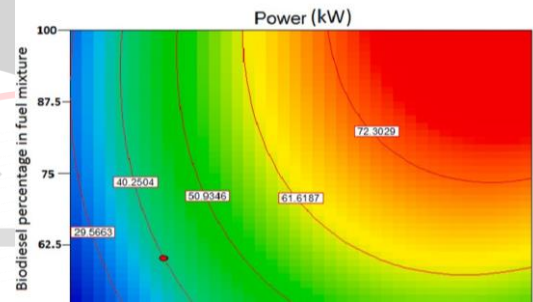


Fig. 10. Brake power versus engine speed at 85% load.

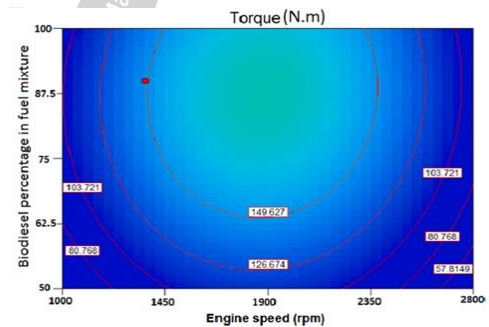


Fig. 11. Torque versus engine speed at 40% load.

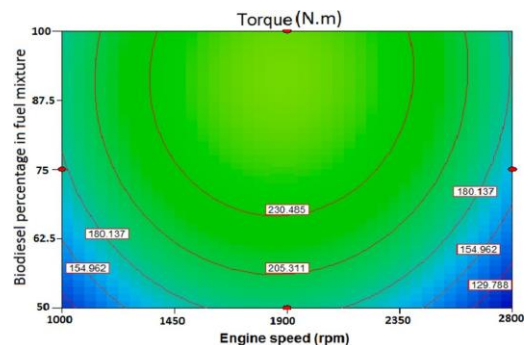


Fig. 12. Torque versus engine speed at 62.5% load.

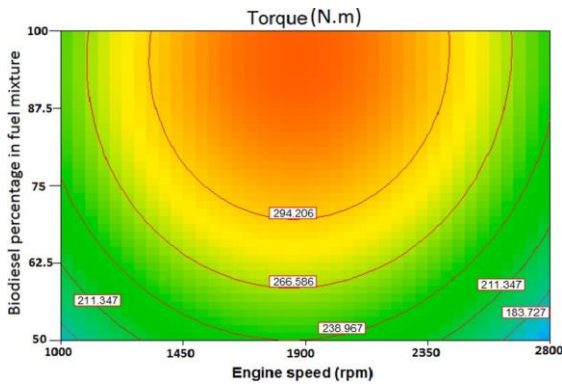


Fig. 13. Torque versus engine speed at 85% load.

Based on the decision parameters, six output parameters including the power, torque, BSFC, CO, NOx, and soot were estimated based on derived mathematical models (Table 7). In order to sum the output parameters, they are normalized into the range of [0, 1] as follows:

$$\begin{aligned}
 f_1 &= (\text{Power} + 0.9213)/97.6413 \\
 f_2 &= (\text{Torque} + 21.7705)/377.7712 \\
 f_3 &= (\text{BSFC} - 202.1308)/137.8924 \\
 f_4 &= (\text{CO} - 0.0074)/0.0530 \\
 f_5 &= (\text{NOx} - 148.7917)/709.2267 \\
 f_6 &= (\text{Soot} - 4.9554)/25.2404
 \end{aligned}
 \tag{4}$$

Finally, the following fitness function is obtained by a linear combination of the output parameters:

$$f = a_1f_1 + a_2f_2 + a_3f_3 + a_4f_4 + a_5f_5 + a_6f_6
 \tag{5}$$

In order to minimize the above fitness function, one should maximize the brake power and torque and minimize the BSFC, CO, NOx, and smoke level, simultaneously. Also, it is desired that CO, NOx, and smoke level are more important than the performance parameters. Therefore, the coefficients of Eq. (5) are selected as follows:

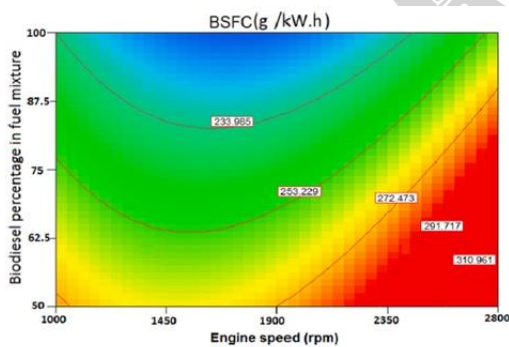


Fig. 14. BSFC versus engine speed at 40% load

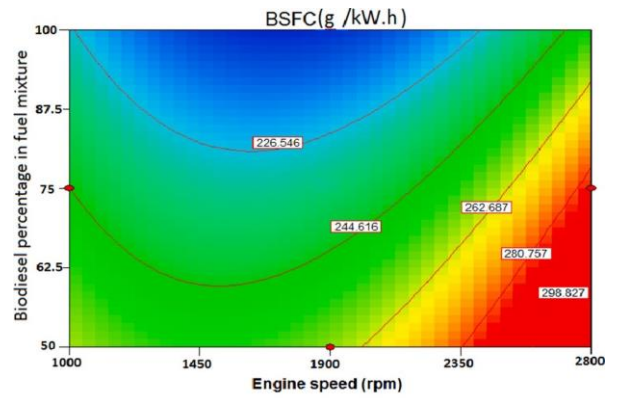


Fig. 15. BSFC versus engine speed at 62.5% load.

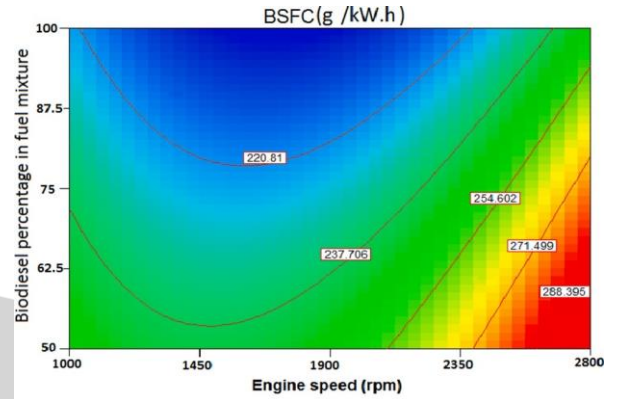


Fig. 16. BSFC versus engine speed at 85% load.

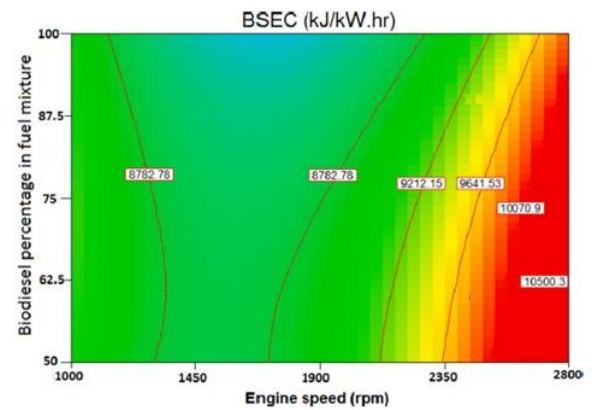


Fig. 17. BSEC versus engine speed at 40% load.

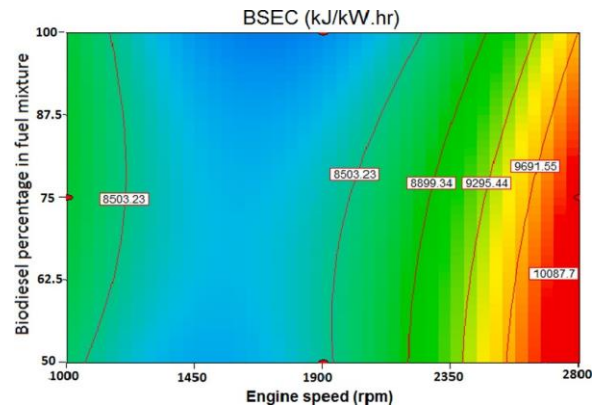


Fig. 18. BSEC versus engine speed at 62.5% load.

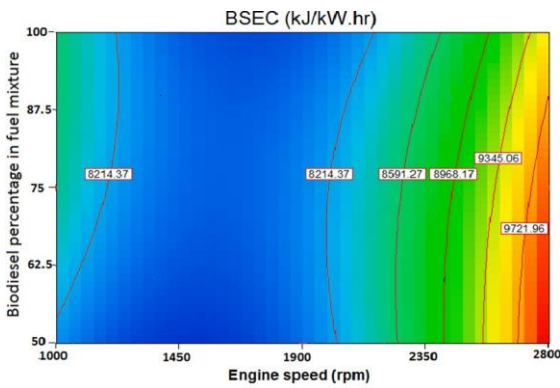


Fig. 19. BSEC versus engine speed at 85% load.

$$a_1 = -1$$

$$a_2 = -1$$

$$a_3 = 1$$

(6)

$$a_4 = 3$$

$$a_5 = 3$$

$$a_6 = 3$$

The GA enhancement calculation is carried out by the MATLAB improvement tool kit. The used GA calculation has the properties introduced in Table 8.

When the GA is executed, the best mix of choice boundaries bringing about the littlest wellness work is acquired. The best wellness work esteem in every age versus emphasis number is introduced in Fig.29. It tends to be seen that the best and mean wellness work esteems at long last unite to 0.307972. In this way, it very well may be reasoned that GA is effective in tracking down the worldwide ideal of the issue.

Additionally, the best individual mixes cause the littlest wellness work esteems in every age versus cycle number is represented in Fig. 30. It very well may be seen the biodiesel rate in the ethanol-biodiesel blend, motor speed, and burden was joined to 94.65%, 2800 RPM, and 65.75%, individually as the ideal conditions. Likewise, the subsequent yield boundaries relating to the littlest wellness work esteems in every age versus cycle number is delineated in Fig. 31. The outcomes are closed in Table 9.

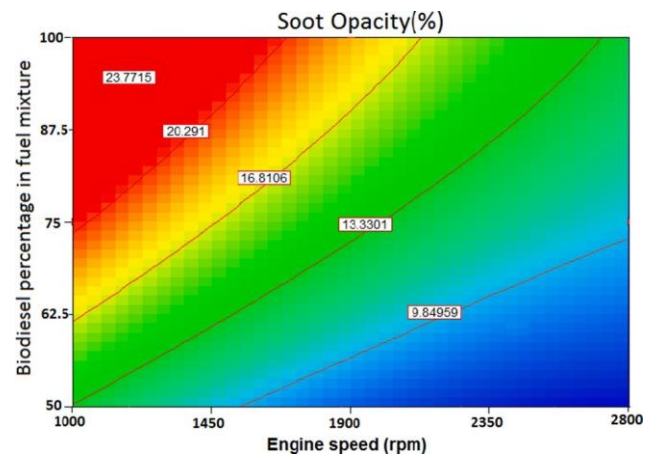


Fig. 21. Smoke level versus engine speed at 62.5% load.

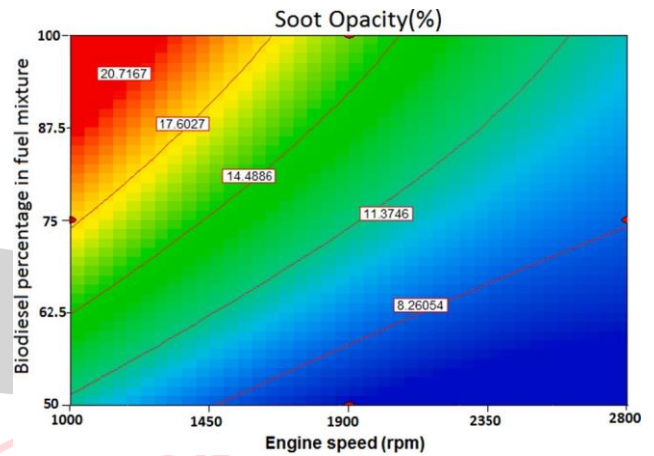


Fig. 22. Smoke level versus engine speed at 85% load.

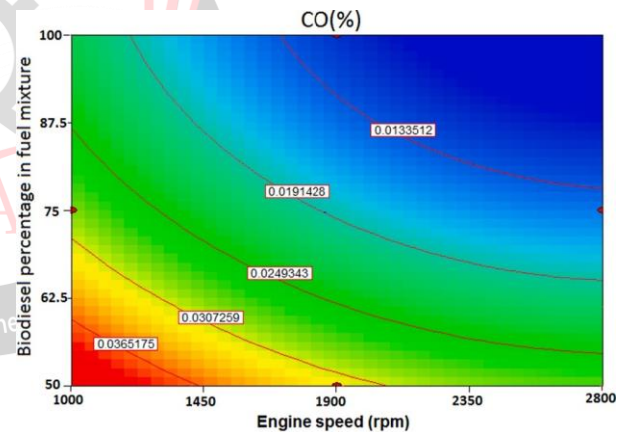


Fig. 23. CO emission versus engine speed at 40% load.

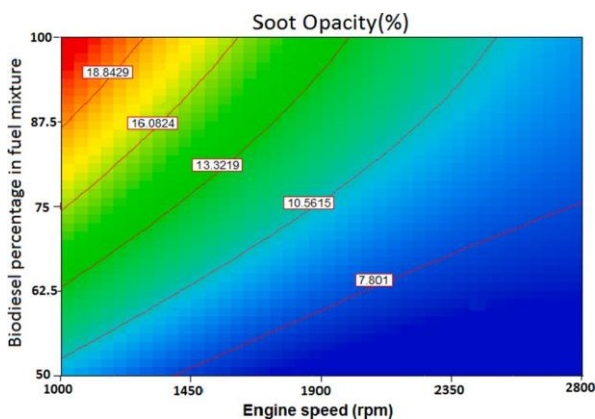


Fig. 20. Smoke level versus engine speed at 40% load.

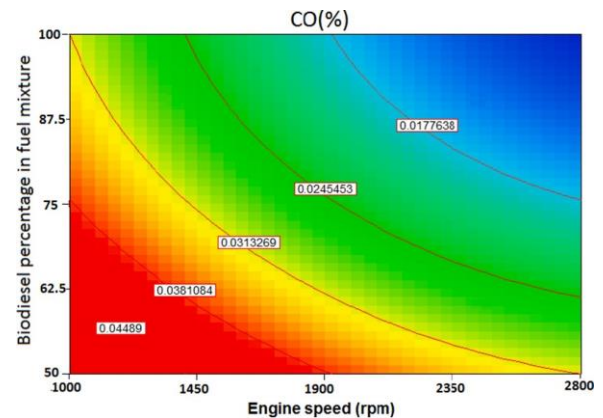


Fig. 24. CO emission versus engine speed at 62.5% load.

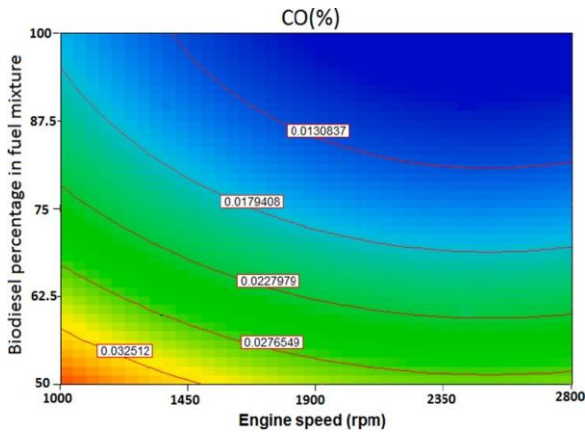


Fig.25.COemissionversusenginespeedat85%load

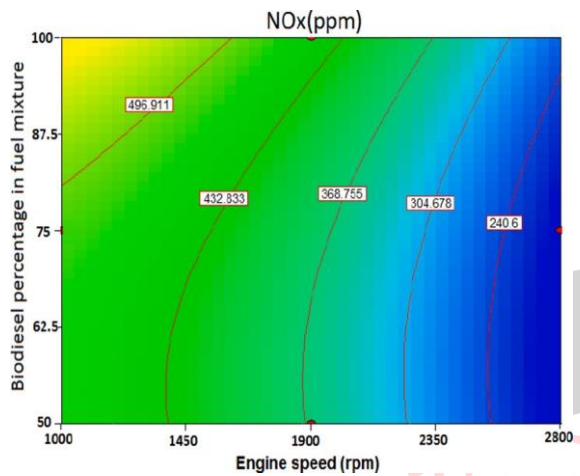


Fig.26. NO_x emission vs engine speed at 40% load.

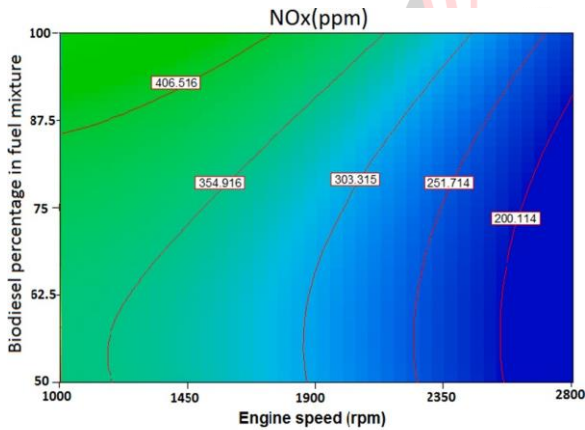


Fig.27.NO_x emission vs engine speed at 62.5% load.

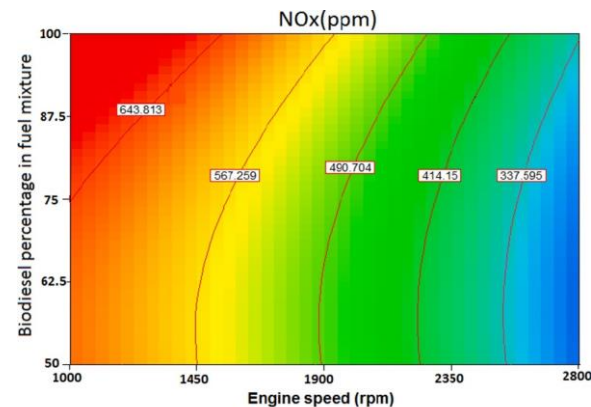


Fig.28. NO_x emission vs engine speed at 85% load.

The experiments were carried at the optimum conditions to validate the optimized results. The average of three measured results was considered as the actual response. The average experimental values, the predicted values, and the percentages of error were presented in Table 10. The validation results demonstrated that the developed models gave an accurate description of the experimental data.

Table 8 The properties of the GA algorithm.

Parameter	Value
Population Size	50
Crossover Fraction	0.8
Elite Fraction	0.05
Migration Fraction	0.2
Penalty Factor	100
Stall Generation Limit	50
Function Tolerance	1e-6
Constraint Tolerance	1e-6
Fitness Scaling	Rank
Selection Function	Stochastic Uniform

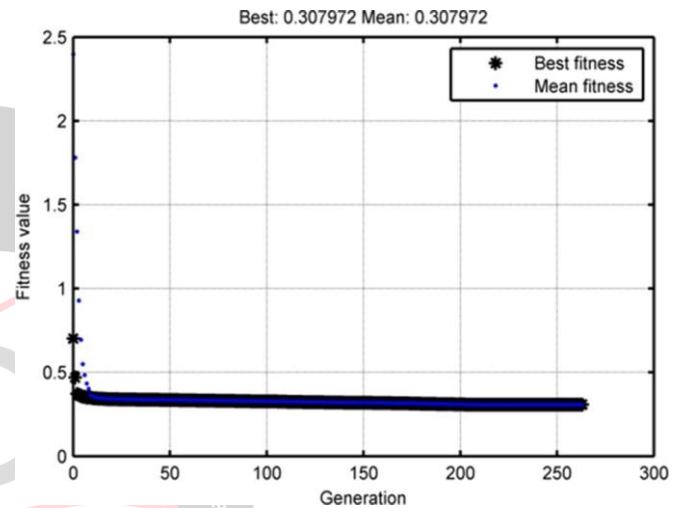


Fig. 29. The best fitness function value in each generation vs iteration number.

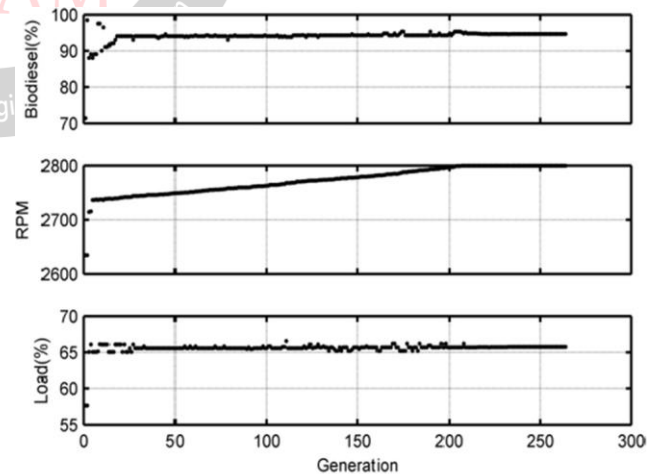


Fig.30. The best individual combinations in each generation vs iteration number.

K. The comparison of the performance and emission characteristics of the biodiesel –ethanol blend with neat diesel

The examination of the exhibition and emanation qualities for B75E25 mix with perfect diesel at the motor speed of 1900 rpm and different motor burdens are portrayed. As indicated by the outcomes, the brake force and force

esteems are lower for B75E25 in examination with diesel fuel on account of the lower energy substance of biodiesel and ethanol contrasted and diesel fuel No.2. Also, the biodiesel-ethanol fuel mix has higher BSFC esteems contrasted and slick diesel. The outcomes likewise showed that the NOx emanations helped up marginally with the utilization of biodiesel-ethanol fuel mix in examination with D100 because of less compressibility, high isentropic mass modulus, and cetane number of biodiesel. Despite the fact that, utilizing ethanol causes impeded burning that decreases ignition temperature and keeps from expanding the NOx outflows. The outcomes likewise showed that the CO outflow and smoke decreased with utilizing B75E25 in correlation with diesel fuel due to oxygen substance in the atomic design of ethanol and biodiesel. As per the outcomes, the distinction between the brake force, force, and BSFC estimations of the B75E25 fuel mix and flawless diesel decline at 85% motor burden. This can be because of the presence of oxygen particles in biodiesel and ethanol structure that prompts higher ignition productivity and makes up for the deficiency of warming estimation of biodiesel and ethanol. Notwithstanding, this pattern has been turned around for discharge boundaries, and the thing that matters is more prominent at high motor burden because of the compelling job of oxygen atoms in diminishing hydrocarbons and carbon monoxide and expanding NOx.

Table9

The results of the GA optimization problem.

Decision Parameters		Output Parameters		Fitness Function	
Parameters	Value	Parameters	Value	Parameters	Value
Biodiesel	95.65%	Brake power(kW)	63.5621	Mean	0.307972
		Brake torque (N.m)	189.1575		
Engine speed (rpm)	2800	BSFC(g/kW.h)	257.9915	Best	0.307972
		Co(%)	0.0084		
load	65.75%	NO _x (ppm)	246.9442		
		Smoke level (soot opacity%)	10.4186		

Table 10 Validation of the GA results.

Biodiesel percentage in fuel mixture (%)	Engine speed (rpm)	Engine load(%)		Brake power (kW)	Brake torque (N.m)	BSFC (gr/Kw.hr)	CO (%)	NO _x (ppm)	Smoke level (%)
94.65%	2800	65.75%	Predicted	63.56	189.16	257.99	0.0084	246.94	10.418
			Actual	60	204	268	0.008	238	10.2
			%Error	4.7	7.8	3.9	4.8	3.6	2.1

IV. CONCLUSION

The essential support this assessment article is to separate the joined impacts of biodiesel-ethanol fuel mixes on the showcase and flood attributes of a diesel motor by the Response Surface Methodology. Thinking about the outcomes, the brake force and force were diminished by around 29% with developing the extent of ethanol in the fuel blend. Possibly than, the BSFC of fuel mixes improved around 15% in with a more raised degree of ethanol considering the lesser calorific appraisal of ethanol related with biodiesel. In any case, higher thickness and thickness of biodiesel premise additional fuel implantation; so there is

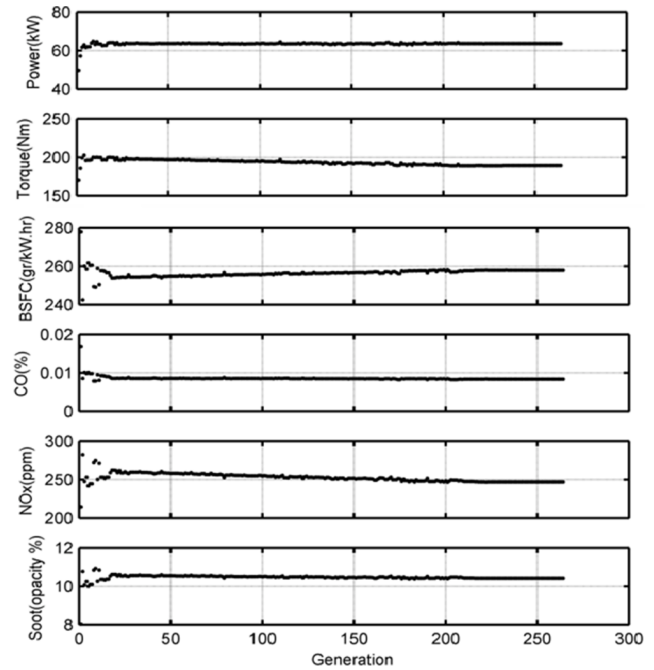


Fig.31. The resulting output parameters corresponding to the smallest fitness function values in each generation vs iteration number.

no recognizable change in BSFC respects for all mixes. About spread restricts, the more level of ethanol accomplished less extent of smoke level and NOx discharge around 38% and 17%, freely considering the mind blowing level of oxygen in the atomic advancement of ethanol. Notwithstanding, there is an around 44% lessening in CO outpourings for a critical level of biodiesel contained mixes. As demonstrated by the GA streamlining, the outcomes showed that the biodiesel rate in the fuel blend, RPM, and motor difficulty were joined to 94.65%, 2800, and 65.75%, in a specific solicitation as the ideal conditions. It is expected that ethanol is more reasonable to improve the spread attributes than that of the presentation qualities.

REFERENCES

- [1] Agarwal AK. Biofuels (alcohols and biodiesel) applications as fuels for internal combustion engines. *Prog Energy Combust Sci* 2007; 33: 233–71.
- [2] Ribeiro NM, Pinto AC, Quintella CM, da Rocha GO, Teixeira LSG, Guarieiro LLN, et al. The Role of Additives for Diesel and Diesel Blended (Ethanol or Biodiesel) Fuels: A Review. *Energy Fuels* 2007; 21: 2433–45.
- [3] Hosseinzadeh Samani B, Ansari Samani M, Shirmeshan A, Fayyazi E, Najafi G, Rostami S. Evaluation of an enhanced ultrasonic-assisted biodiesel synthesized using safflower oil in a diesel power generator. *Biofuels* 2020; 11: 523–32.
- [4] Aydın F, Ögüt H. Effects of using ethanol-biodiesel-diesel fuel in single cylinder diesel engine to engine performance and emissions. *Renewable Energy* 2017; 103: 688–94.
- [5] Madiwale S, Karthikeyan A, Bhojwani V. Properties investigation and performance analysis of a diesel engine fuelled with Jatropha, Soybean, Palm and Cottonseed biodiesel using Ethanol as an additive. *Mater Today: Proc* 2018; 5:657–64.
- [6] Shaafi T, Velraj R. Influence of alumina nanoparticles, ethanol and isopropanol blend as additive with diesel-soybean biodiesel blend fuel: Combustion, engine performance and emissions. *Renewable Energy* 2015; 80:655–63.
- [7] Abdelmalek Z, Alamian R, Safdari Shadloo M, Maleki A, Karimipour A. Numerical study on the performance of a homogeneous charge compression ignition engine fueled with different blends of biodiesel. *J Therm Anal Calorim* 2020.
- [8] Singh A, Sinha S, Choudhary AK, Panchal H, Elkelawy M, Sadasivuni KK. Optimization of performance and emission characteristics of CI engine fueled with Jatropha biodiesel produced using a heterogeneous catalyst (CaO). *Fuel* 2020; 280: 118611.
- [9] Elkelawy M, Bastawissi H-A-E, Esmaeil KK, Radwan AM, Panchal H, Sadasivuni KK, et al. Maximization of biodiesel production from sunflower and soybean oils and prediction of diesel engine performance and emission characteristics through response surface methodology. *Fuel* 2020; 266:117072.
- [10] Elkelawy M, Kabeel A E, El Shenawy E A, Panchal H, Elbanna A, Bastawissi H-A-E, et al. Experimental investigation on the influences of acetone organic compound additives into the diesel/biodiesel mixture in CI engine. *Sustainable Energy Technol Assess* 2020; 37:100614.
- [11] Elkelawy M, Etaiw SE-dH, Bastawissi HA-E, Marie H, Elbanna A, Panchal H, Sadasivuni K, Bhargav H. Study of diesel-biodiesel blends combustion and emission characteristics in a CI engine by adding nanoparticles of Mn (II) supramolecular complex. *Atmospheric Pollution Res* 2020; 11:117–28.
- [12] Zheng Z, Wang X, Zhong X, Hu B, Liu H, Yao M. Experimental study on the combustion and emissions fueling biodiesel/n-butanol, biodiesel/ethanol and biodiesel/2,5- dimethylfuran on a diesel engine. *Energy* 2016; 115:539–49.
- [13] Zheng Z, Xia M, Liu H, Wang X, Yao M. Experimental study on combustion and emissions of dual fuel RCCI mode fueled with biodiesel/n-butanol, biodiesel/2,5- dimethylfuran and biodiesel/ethanol. *Energy* 2018; 148:824–38.
- [14] Tutak W, Jamrozik A, Pyrc M, Sobiepan´ski M. A comparative study of co combustion process of diesel-ethanol and biodiesel-ethanol blends in the direct injection diesel engine. *Appl Therm Eng* 2017; 117:155–63.
- [15] Hu N, Tan J, Wang X, Zhang X, Yu P. Volatile organic compound emissions from an engine fueled with an ethanol-biodiesel-diesel blend. *J Energy Inst* 2017; 90:101–9.
- [16] Aydın H, İklilç C. Effect of ethanol blending with biodiesel on engine performance and exhaust emissions in a CI engine. *Appl Therm Eng* 2010; 30:1199–204.
- [17] Hulwan DB, Joshi SV. Performance, emission and combustion characteristic of a multi cylinder DI diesel engine running on diesel–ethanol–biodiesel blends of high ethanol content. *Appl Energy* 2011; 88:5042–55.
- [18] No SY. A Review on Spray Characteristics of Bioethanol and Its Blended Fuels in CI Engines. *J ILASS-Korea* 2014; 19:155–66.
- [19] Bhowmik S, Paul A, Panua R, Ghosh SK, Debroy D. Performance-exhaust emission prediction of diesolenol fueled diesel engine: An ANN coupled MORSM based optimization. *Energy* 2018; 153:212–22.
- [20] Montgomery DC. Design and analysis of experiments. John Wiley & Sons; 2008.
- [21] Amiri M, Shirmeshan A. Effects of air swirl on the combustion and emissions characteristics of a cylindrical furnace fueled with diesel-biodiesel-n-butanol and diesel biodiesel-methanol blends. *Fuel* 2020; 268:117295.
- [22] Motamedifar N, Shirmeshan A. An experimental study of emission characteristics from cylindrical furnace: Effects of using diesel-ethanol-biodiesel blends and air swirl. *Fuel* 2018; 221:233–9.
- [23] Ozsezen AN, Canakci M, Turkan A, Sayin C. Performance and combustion characteristics of a DI diesel engine fueled with waste palm oil and canola oil methylesters. *Fuel* 2009; 88:629–36.
- [24] Dwivedi G, Sharma MP, Verma P, Kumar P. Engine Performance Using Waste Cooking Biodiesel and Its Blends with Kerosene and Ethanol. *Mater Today: Proc* 2018; 5:22955–62.
- [25] Fazal M A, Haseeb A S M A, Masjuki H H. A critical review on the tribological compatibility of automotive materials in palm biodiesel. *Energy Convers Manage* 2014; 79:180–6.
- [26] Rakopoulos DC, Rakopoulos CD, Kakaras EC, Giakoumis EG. Effects of ethanol–diesel fuel blends on the performance and exhaust emissions of heavy duty DI diesel engine. *Energy Convers Manage* 2008; 49:3155–62.
- [27] Roskilly A, Nanda S, Wang Y, Chirkowski J. The performance and the gaseous emissions of two small marine craft diesel engines fuelled with biodiesel. *Appl Therm Eng* 2008; 28:872–80.
- [28] Rakopoulos DC, Rakopoulos CD, Papagiannakis RG, Kyritsis DC. Combustion heat release analysis of ethanol or n-butanol diesel fuel blends in heavy-duty DI diesel engine. *Fuel* 2011; 90:1855–67.
- [29] Ghani IA, Sidic NAC, Mamat R, Najafi G, Ken TL, Asako Y, Japar WMAA. Heat transfer enhancement in microchannel heat sink using hybrid technique of ribs and secondary channels. *Int J Heat Mass Transfer* 2017; 114:640–55